



## Efimov effect and three-body decay

A.S. Jensen<sup>a</sup>, D.V. Fedorov<sup>a</sup>, R. Alvarez-Rodriguez<sup>a</sup>, E. Garrido<sup>b</sup>

<sup>a</sup>Department of Physics and Astronomy, University of Aarhus, DK-8000 Aarhus C

<sup>b</sup>Instituto de Estructura de la Materia, CSIC, E-28006 Madrid

The Efimov effect is discussed by use of hyperspherical coordinates and adiabatic potentials. The energy and size scalings are very sensitive to the two independent mass ratios. Two large and one small mass provide the smallest energy spacing. It is less important whether two or three scattering lengths are large. Energy distributions arising from three-body decays are computed for one resonance in  $^{12}\text{C}$  and for the predicted  $^{11}\text{Li}$   $1^-$ -resonance. The decaying  $^{11}\text{Li}$  three-body system with three large  $s$ -wave scattering lengths exhibits characteristic peaks in the energy distribution. This may be considered as a signature of the Efimov effect in similar nuclear three-body decays.

### 1. INTRODUCTION

Consequences of the Efimov effect [1] have recently been observed in a three-body recombination process occurring in an ultracold gas of cesium atoms [2]. This three-body continuum effect was predicted before the experiment [3]. Possible Efimov states in two-neutron halos were discussed in [4] by use of the Faddeev equations in coordinate space [5]. Occurrence in nuclear physics was concluded to be very unlikely in contrast to appearance in atomic and molecular physics [6]. The reason is essentially that asymmetric molecular systems exist and rather easily can be made [7].

In nuclear physics more and more accurate and kinematically complete experiments on decay properties appear in the literature [8]. Also corresponding theoretical formulations and computations are published [9]. One surprising conclusion is that the resonances rather easily change structure from small to large distance, where the  $s$ -waves are favored at large distance. This is reminiscent of the Efimov effect originating in coherent contributions from different two-body  $s$ -wave attractions at large distance. This anomaly can be described in analytical details for  $s$ -waves with square well potentials [10] and in general for higher angular momenta [11]. Recently the features characteristic for the energy distributions after three-body decay were investigated for systems with large  $s$ -wave scattering lengths which precisely is the condition for occurrence of the Efimov effect [12]. In this report we first present optimum conditions for the Efimov effect in terms of the particle masses, and second we discuss computed energy distributions for one  $^{12}\text{C}$  resonance, and finally we discuss traces of the Efimov effect in one  $^{11}\text{Li}$  resonance.

## 2. CONDITIONS FOR THE EFIMOV EFFECT

The masses and the coordinates of the three particles are  $m_i$  and  $\mathbf{r}_i$ , where  $i = 1, 2, 3$ . The particles are then labeled by a permutation,  $(i, j, k)$ , of  $(1, 2, 3)$ . We choose hyperspherical coordinates where we here only need to define the hyperradius  $\rho$ :

$$\rho^2 \equiv \frac{1}{mM} \sum_{i < j} m_i m_j (\mathbf{r}_i - \mathbf{r}_j)^2 \quad ; \quad M = m_i + m_k + m_j, \quad (1)$$

where  $m$  is a normalization mass. All other coordinates are dimensionless angles  $\Omega$ .

### 2.1. Adiabatic potentials and wavefunctions

We employ the hyperspherical expansion method which, combined with complex scaling of the coordinates, provides both bound states and resonances. This means that we, with a given set of interactions, solve the Faddeev equations for each fixed  $\rho$  leading to angular eigenvalues  $\lambda_n(\rho)$  and eigenfunctions  $\Phi_n(\rho, \Omega)$ . The three-body bound state or resonance wave function  $\Psi$  is then

$$\Psi(\rho, \Omega) = \sum_n \frac{f_n(\rho)}{\rho^{5/2}} \Phi_n(\rho, \Omega) = \sum_n \frac{f_n(\rho)}{\rho^{5/2}} \left( \phi_1^{(n)}(\rho, \Omega) + \phi_2^{(n)}(\rho, \Omega) + \phi_3^{(n)}(\rho, \Omega) \right), \quad (2)$$

where the amplitudes,  $f_n(\rho)$ , are the radial wave functions.

We restrict ourselves to only  $s$ -waves which describe the Efimov effect when at least two scattering lengths  $a_{ij}$  are large compared to the effective ranges  $R_{ij}$ . At intermediate distances the adiabatic potential  $U$ , determining  $f_n$ , has the generic form for producing Efimov states [1,11,7]

$$U(\rho) = -\frac{\hbar^2}{2m} \left( \frac{\xi^2 + 1/4}{\rho^2} \right) \quad \text{for } R_{av} \leq \rho \leq a_{av} \quad ; \quad U(\rho) = \frac{\hbar^2}{2m\rho^2} \frac{48}{\pi\sqrt{2}} \frac{a_{av}}{\rho} \quad \text{for } a_{av} \leq \rho, \quad (3)$$

where  $\xi^2$  is a constant depending on interactions and masses. The averages of scattering lengths and effective ranges are defined by

$$a_{av}\sqrt{m} \equiv \frac{\sqrt{2}}{3} \sum_{i < k} \sqrt{\mu_{ik}} a_{ik} \quad ; \quad R_{av}\sqrt{m} \equiv \frac{\sqrt{2}}{3} \sum_{i < k} \sqrt{\mu_{ik}} R_{ik} \quad ; \quad \mu_{ik} = m_i m_k / (m_i + m_k). \quad (4)$$

At small  $\rho$ ,  $U(\rho)$  is strongly interaction dependent.

The radial wave functions,  $f_n$ , determined by the potentials are given by [13]

$$f_n \propto \sqrt{\rho} \sin \left( \xi \ln \left( \frac{\rho}{R_{av}} \right) \right) \quad \text{for } \kappa_n \rho < 1 \quad ; \quad f_n \propto \exp(-\kappa_n \rho) \quad \text{for } \kappa_n \rho > 1, \quad (5)$$

where the energy is given by  $E_n = -\hbar^2 \kappa_n^2 / (2m)$ . The exponential decrease at large distance signals a bound state. The radial wavefunction  $f_n$  oscillates periodically with  $\rho$  as  $\sin(\xi \ln \rho)$ . We assumed that the zero point for the first oscillation is given by  $R_{av}$ .

The number of Efimov states  $N_E$  is found as the number of oscillations between  $R_{av}$  and  $48a_{av}/(\pi\sqrt{2}) \approx 11a_{av}$  [13], i.e.

$$N_E \approx \frac{\xi}{\pi} \ln \left( \frac{11a_{av}}{R_{av}} \right). \quad (6)$$

The energies and sizes of these states are related by

$$\frac{E_n}{E_{n+1}} = \frac{\langle \rho^2 \rangle_{n+1}}{\langle \rho^2 \rangle_n} = \exp(2\pi/\xi), \quad (7)$$

where the exponential behavior originates from the  $1/\rho^2$  potential in eq.(3).

## 2.2. Mass dependence of the potential strength

The strength  $\xi$  in eq.(3) is found from equations depending on the mass ratios. When the Pauli principle is inactive, three identical Fermions are excluded, we obtain the equation for  $\xi$  for three large scattering lengths [10]

$$\left( \frac{\xi \cosh(\xi\pi/2)}{2G} \right)^3 - \frac{\xi \cosh(\xi\pi/2)}{2G} \frac{(g_1^2 + g_2^2 + g_3^2)}{G^2} - 2 = 0, \quad (8)$$

where the functions  $g_k$  depend on  $\xi$  and the angles  $\varphi_k$  depend on two independent mass ratios, i.e.

$$g_k = \frac{\sinh(\xi(\pi/2 - \varphi_k))}{\sin(2\varphi_k)}; \quad G = (f_1 f_2 f_3)^{1/3}; \quad \varphi_k = \arctan \left( \sqrt{\frac{m_k(m_1 + m_2 + m_3)}{m_i m_j}} \right). \quad (9)$$

When all masses are equal  $G = g_1 = g_2 = g_3$  and eq.(8) reduces to two independent equations, i.e.

$$8 \sinh(\xi\pi/6) = \xi \sqrt{3} \cosh(\xi\pi/2); \quad -4 \sinh(\xi\pi/6) = \xi \sqrt{3} \cosh(\xi\pi/2), \quad (10)$$

where the first equation is the celebrated Efimov equation for identical bosons with the solution  $\xi \simeq 1.0063$  independent of the particle masses. The second equation has no real solutions  $\xi$  and consequently no bound states exist for the potential in eq.(3).

If only two scattering lengths are large ( $a_{jk}$  and  $a_{ik}$ , not  $a_{ij}$ ), the coherence leading to the expression for the strength is instead given by

$$\xi \cosh(\xi\pi/2) \sin(2\varphi_k) = 2 \sinh(\xi(\pi/2 - \varphi_k)), \quad (11)$$

where  $\xi$  now only depends on  $\varphi_k$ . With only one large scattering length the Efimov effect does not appear.

The transcendental equation for the strength  $\xi$ , obtained from eqs.(8), (10) or (11), show dependence of two mass ratios, e.g.  $m_2/m_1$  and  $m_3/m_1$ , through eq.(9). Pronounced Efimov effect occurs for large  $\xi$ , i.e. the energy spacing between states is small and the size increase is correspondingly large as expressed precisely in eq.(7). This is shown in fig.1 where the three diverging corners are related to one of the masses being small compared to both the other masses. The values of  $\xi$  are moderate for nearly identical masses while exceedingly large  $\xi$ -values are possible for very asymmetric systems.

These considerations are only valid if at least two scattering lengths are much larger than the effective ranges. Otherwise the Efimov effect does not occur at all. Strictly, we assumed all three lengths to be large but the effect of the mass asymmetry is much more important than contributions from two or three scattering lengths as seen by comparing solutions to eqs.(8), (10) or (11). This is an advantage since two identical particles immediately implies two identical (large or small) scattering lengths. More luck or technical

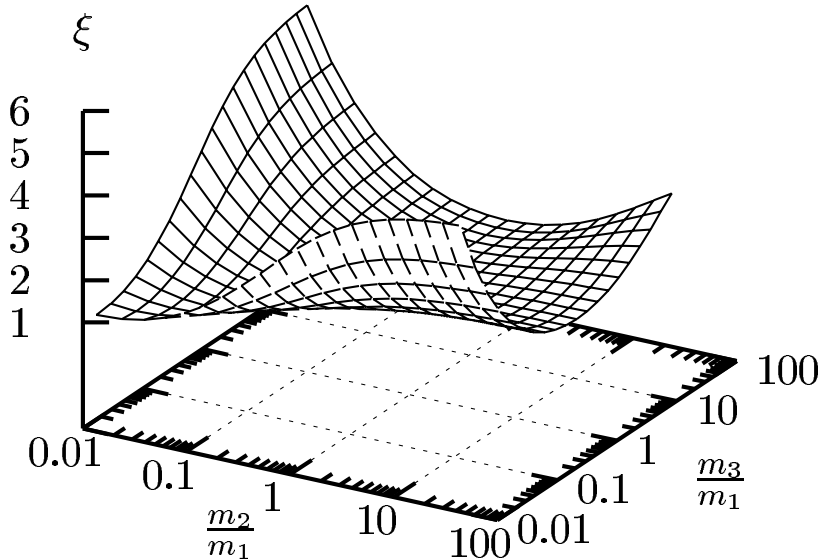


Figure 1. Three-dimensional plot of the strength parameter  $\xi$  obtained from eq.(8).

skills are required if two independent scattering lengths simultaneously has to be large. Three identical bosons are then a disadvantage due to the much smaller effect even though systems with three identical scattering lengths presumably are easier to find.

Favorable mass ratios are obtained by one electron and two atoms, but one light atom and two (maybe identical) atoms is also rather favorable. In contrast, nuclear clusters always involve long-range Coulomb interactions ( $1/r$ -behavior) which spoils the decisive  $1/\rho^2$ -behavior at large distance. Thus only two neutrons and a core-nucleus is a possible combination in nuclear physics. Unfortunately this means two light and one heavy particle which at best produces very small  $\xi$ -values.

### 3. THE ENERGY DISTRIBUTIONS AFTER RESONANCE DECAY

Three-body decay is a three-body problem at large distance. We mock up the effects of other, perhaps decisive, degrees of freedom at smaller distances by using a three-body short-range interaction. We apply this generalization of  $\alpha$ -emission to three-body decay of resonances.

The complex energy  $E_0$  of a three-body resonance is given by

$$E_0 = E_r - i\frac{\Gamma_r}{2} = \frac{\hbar^2 \kappa_0^2}{2m}, \quad (12)$$

where the corresponding asymptotic coordinate and momentum wave functions have the forms [9]

$$\Psi_{\kappa_0}(\rho, \Omega_\rho) \rightarrow \rho^{-5/2} \exp(i\kappa_0 \rho) \Phi(\Omega), \quad \Psi_\kappa(\Omega_\kappa) \rightarrow \frac{2(2\pi)^{5/2} \Phi(\kappa, \Omega_\kappa)}{\kappa_0^{3/2} \kappa^2 - \kappa_0^2}, \quad (13)$$

where  $\Omega_\kappa$  denotes the (hyper)angles related to the conjugate momenta. The energy is shared between the three particles according to this momentum-space expression.

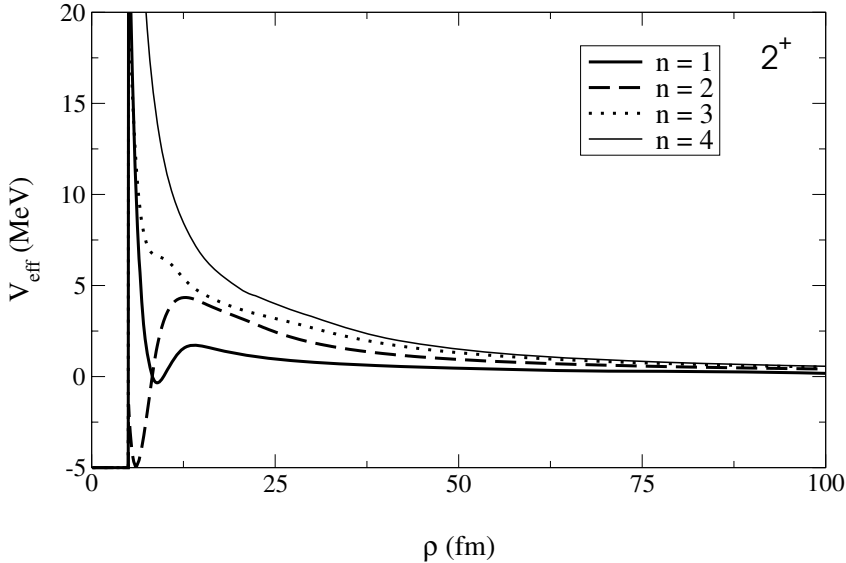


Figure 2. The real parts of the 4 lowest adiabatic effective potentials as functions of  $\rho$  for the  $2^+$ -states in  $^{12}\text{C}$  ( $\alpha + \alpha + \alpha$ ).

### 3.1. The three- $\alpha$ model of $^{12}\text{C}$

We illustrate by  $2^+$ -resonances in  $^{12}\text{C}$  decaying into three  $\alpha$ -particles. The adiabatic potentials shown in fig.2 are first computed. The attractive pockets at small distance, supplemented by the three-body interaction, support one bound state and several resonances. Their energies can easily be adjusted by three-body interactions with a range comparable to the extension of the three-body system. This implies that the widths essentially are determined by the tunneling probability through the barriers in fig.2. The energy distribution between the  $\alpha$ -particles is determined by the properties of the large-distance asymptotic wave function in eq.(13), see [14] for computational details.

The radial equations now provide continuum solutions and corresponding energies as shown in fig.3. The region resembling an uncertain straight line are ordinary oscillating discretized continuum states. The black squares are bound states ( $E_R < 0, E_I = 0$ ) and resonances with bound state asymptotic boundary conditions. Their structures are essentially determined by the three lowest diagonal effective potentials in fig.2. Except for the highest-lying resonance all states are experimentally established and the corresponding widths are consistent with measurements.

The energy distributions of the  $\alpha$ -particles are now computed from eq.(13) and shown in fig.4 for the third  $2^+$  state at 7.4 MeV. The peak close to maximum energy corresponds to sequential decay via the  $0^+$  ground-state of  $^8\text{Be}$  which in turn decays into  $\alpha$ -particles which appear with energies at around 0.25. Sequential decay via the  $2^+$  state of  $^8\text{Be}$  produces a peak at around 0.38. The subsequent decay of the  $2^+$ -state produce a distribution ranging from about 0.04 to 0.85. Whether the combination of these sequential decays can account for all details of the distribution is still an open question. Possibly also a fraction of direct decay is needed.

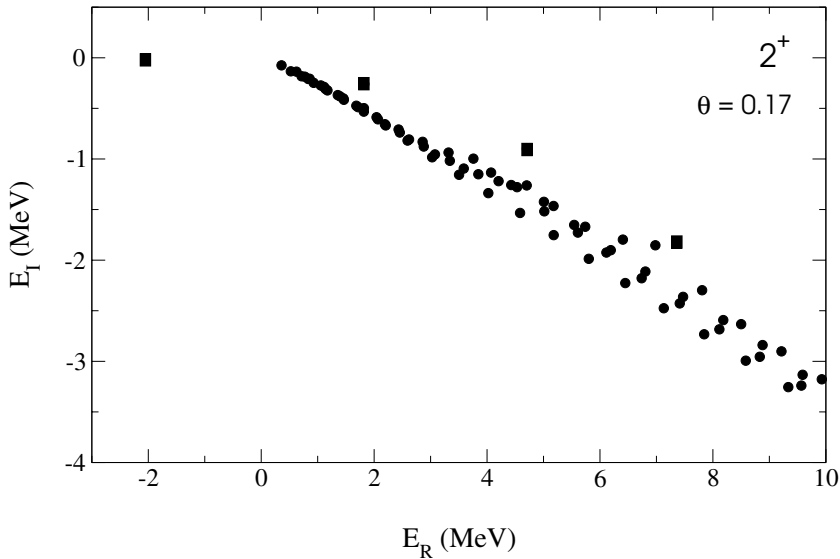


Figure 3. The real and imaginary parts of the computed three-body energies in  $2^+$ -states in  $^{12}\text{C}$  after complex scaling by an angle  $\theta = 0.17$ . The filled circles are discretized continuum states and the filled squares are bound states and resonances.

### 3.2. Two-neutron halos: $^{11}\text{Li}$

The Efimov effect producing more than one state with the proper scaling properties is not expected in nuclei since only two-neutron structures around a core has the necessary short-range interaction. However, excited states can also exhibit characteristic Efimov features, and furthermore three-body decay of resonances could leave some trace of the effect. The reason is that a three-body resonance produced by attraction in higher partial waves than  $l = 0$  easily can have  $s$ -wave character at larger distances. This change of structure from small to large distance arises since effective  $s$ -wave potentials fall off slower with distance than all other potentials. The resonance wave function then either has to follow the lowest potential energy (adiabatic) or maintain its structure (diabatic). The chance of seeing the Efimov effect is enhanced when  $s$ -waves extend to large distances. Coherent contributions from  $s$ -waves in different Jacobi coordinates are required.

The decay of the  $1^-$ -resonance in  $^{11}\text{Li}$  is used as illustration in fig.5. The  $s$ -wave interaction produces rather clear peaks in the spectra, i.e. (i) emission of one neutron leaving a neutron-core system (favored by their  $s$ -wave attraction) provides both a high and a low neutron-energy peak while the  $\alpha$ -particle has a peak at intermediate energy, (ii)  $\alpha$ -emission leaving two neutrons behind (favored by their  $s$ -wave attraction) provides the intermediate energy neutron peak and the high-energy  $\alpha$ -particle peak. These characteristic features, arising from contributions of different  $s$ -waves, remain in the results for realistic interactions reproducing all other known  $^{11}\text{Li}$  properties. The relative peak heights are changed and the intermediate neutron-energy peak has almost disappeared.

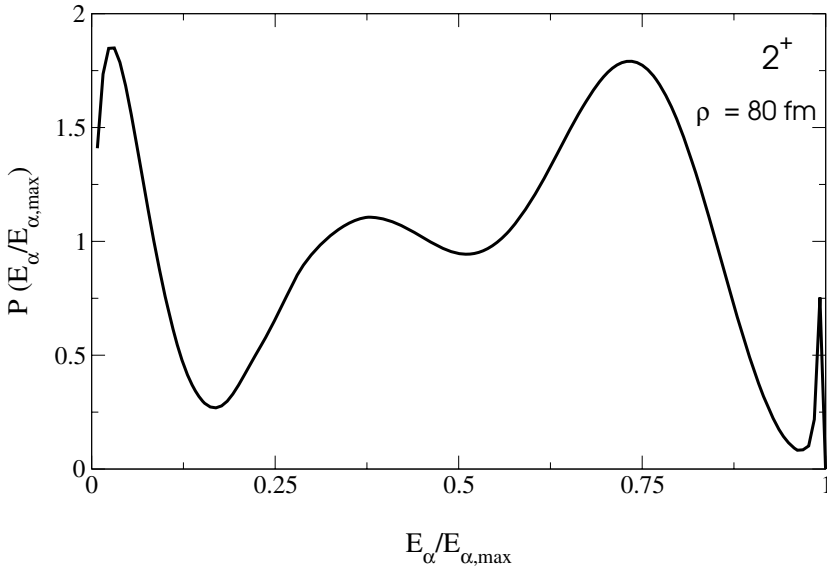


Figure 4. The energy distribution of the individual  $\alpha$ -particles appearing after decay of the third  $2^+$ -resonance in  $^{12}\text{C}$ , see [14] for computational details.

Traces of the Efimov effect seems to stay in these three-body decays where all three  $s$ -wave scattering lengths are large.

#### 4. CONCLUSIONS

The Efimov effect produces bound three-body states with relatively small energy spacing and size variation when one of the masses is much smaller than the other two masses. In any case at least two of the  $s$ -wave scattering lengths must be large. The long-range Coulomb interaction spoils the effect. In nuclear physics this leaves only two neutrons outside a charged nucleus which unfortunately has an unfavorable set of mass ratios. Atomic and molecular physics provide much more favorable systems as demonstrated experimentally in the three-body recombination found in an ultracold gas of cesium atoms.

In nuclear physics the recent accurate and kinematically complete experiments provide energy distributions after three-body decay of resonances for example populated in beta-decay. When the  $s$ -wave parts of the two-body interactions have large scattering lengths the decay may exploit the energetically favorable  $s$ -waves at large distances even when the short-distance structure is dominated by higher partial waves. The adiabatic-diabatic competition between low energy and maintaining structure may then lead to Efimov-like resonance structures at large distances. This in turn would produce characteristic energy distributions of the three particles after the decay. Realistic interactions would probably smear out the schematic structure but possibly leave significant traces of the Efimov effect in such decays.

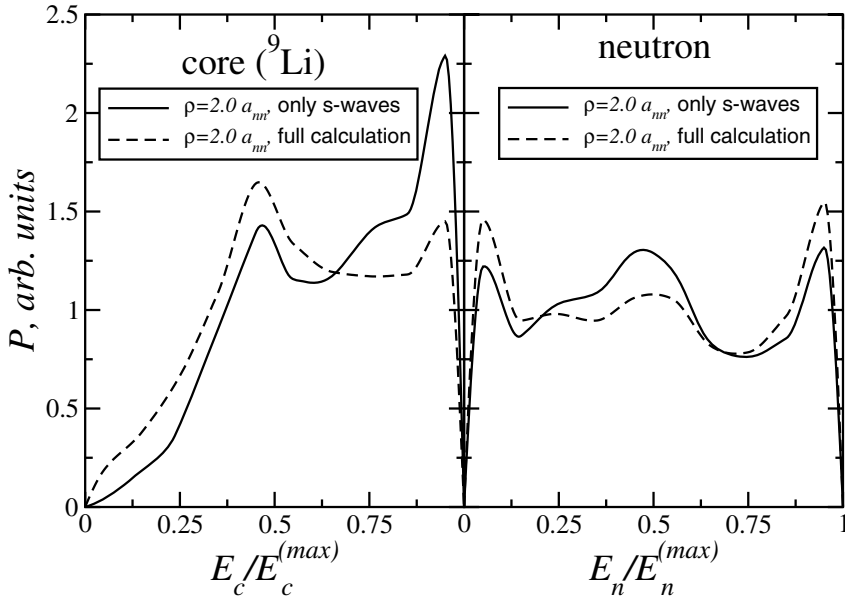


Figure 5. Energy distributions of the fragments - the core,  ${}^9\text{Li}$ , and the neutrons - in the decay of the  $(1^-)$  three-body resonance in  ${}^{11}\text{Li}$  calculated with interactions where the neutron-core and neutron-neutron scattering lengths are about 20 fm. Both schematic (only  $s$ -waves) and realistic (all partial waves) results are shown.

## REFERENCES

1. V. Efimov, Phys. Lett. 33B (1970) 563.
2. T. Kraemer et al., Nature 440 (2006) 315.
3. B.D. Esry, C.H. Greene, J.P. Burke Jr., Phys. Rev. Lett. 83 (1999) 1751.
4. D.V. Fedorov, A.S. Jensen and K. Riisager, Phys. Rev. Lett. 73 (1994) 2817.
5. D. V. Fedorov and A. S. Jensen, Phys. Rev. Lett. 71 (1993) 4103.
6. A.S. Jensen et al., Rev. Mod. Phys. 76 (2004) 215.
7. A.S. Jensen and D.V. Fedorov, Europhysics Lett. 62 (2003) 336.
8. B. Blank, J. Giovanazzo and M. Pfützner, C.R. Physiques 4 (2003).
9. E. Garrido et al., Nucl. Phys. A748 (2005) 27, 39; *ibid* A766 (2006) 74.
10. A.S. Jensen, E. Garrido and D.V. Fedorov, Few-Body Systems 22 (1997) 193.
11. E. Nielsen, D.V. Fedorov, A.S. Jensen and E. Garrido, Phys. Rep. 347 (2001) 373.
12. E. Garrido, D.V. Fedorov and A.S. Jensen, Phys. Rev. Lett. 96 (2006) 112501.
13. E. Nielsen, D.V. Fedorov and A.S. Jensen, J. Phys. B31 (1998) 4085.
14. D.V. Fedorov et al., Few-Body Systems 34 (2004) 33.